

Influence of Extra Neutrons Added to the $^{12}\text{C} + ^{16}\text{O}$ System: Gross Structures in γ -Ray Yields Following the $^{13}\text{C} + ^{16}\text{O}$ and $^{12}\text{C} + ^{18}\text{O}$ Reactions

Y.-d. Chan, H. Bohn,^(a) R. Vandenbosch, R. Sielemann,^(b) J. G. Cramer, K. G. Bernhardt,^(c)
H. C. Bhang, and D. T. C. Chiang

Nuclear Physics Laboratory, University of Washington, Seattle, Washington 98195

(Received 26 December 1978)

Excitation functions for the dominant fusion channels in the $^{13}\text{C} + ^{16}\text{O}$ and $^{12}\text{C} + ^{18}\text{O}$ reactions have been measured from 7 to 25 MeV (c.m.) using γ -ray spectroscopy. Comparison with the $^{12}\text{C} + ^{16}\text{O}$ system shows that gross structure persists in the α -out channel for $^{13}\text{C} + ^{16}\text{O}$ but is not apparent in this channel for $^{12}\text{C} + ^{18}\text{O}$, although observed in the inelastic channels for the latter. $^{13}\text{C} + ^{16}\text{O}$ is the first system not comprised of α -cluster nuclei to exhibit gross structures in fusion channels.

Since the first observation of regular gross structures in the total fusion excitation functions¹ for $^{12}\text{C} + ^{16}\text{O}$ and $^{12}\text{C} + ^{12}\text{C}$ many studies have been devoted to further investigation of this phenomenon. The origin of these structures is still not clear. In order to obtain a better understanding of the systematics and exit-channel dependence of these structures we have measured the γ -ray yields following the $^{13}\text{C} + ^{16}\text{O}$ and $^{12}\text{C} + ^{18}\text{O}$ reactions, corresponding to the addition of one and two extra neutrons to the $^{12}\text{C} + ^{16}\text{O}$ system. We report in this Letter the first evidence for regular gross structures in the fusion channel ($\alpha + ^{25}\text{Mg}$) for a system ($^{13}\text{C} + ^{16}\text{O}$) not comprised of α -cluster reactants in the entrance channel, and show how there is a systematic attenuation of the structures in the α -out channel as neutrons are added to the $^{12}\text{C} + ^{16}\text{O}$ system. Our particular emphasis is placed on the results for the α -out exit channels since these channels have been shown to be the most sensitive indication of structures in the fusion cross sections.²⁻⁵ No results on the fusion cross section for $^{13}\text{C} + ^{16}\text{O}$ (involving an odd- N nucleus in the entrance channel) have been published while γ -ray measurements for the $^{12}\text{C} + ^{18}\text{O}$ reaction have been reported recently by Freeman and Haas.⁶

The experimental setup and procedures are similar to our previous $^{12}\text{C} + ^{16}\text{O}$ measurement.⁵ Targets were prepared by evaporating isotopic (99.8% purity) ^{12}C and ^{13}C layers of $\sim 100\text{-}\mu\text{g}/\text{cm}^2$ thickness onto thick metallic tantalum (98 mg/cm²) backing foils. The effective mean target thickness was about 285 keV (c.m.) at $E_{\text{c.m.}} = 8$ MeV and 180 keV at $E_{\text{c.m.}} = 27$ MeV for ^{16}O particles. This was sufficient to damp out any Ericsson fluctuations. One or two 60-cm³ coaxial Ge(Li) detectors have been used to detect the reaction γ rays in singles mode. The number of beam particles for each run during the experiment was ob-

tained by integrating the beam current on target. The absolute cross section is estimated to be accurate to within 30%. More details can be found in Ref. 5.

In the case of the $^{13}\text{C} + ^{16}\text{O}$ reaction, γ rays were detected at $\theta_{\gamma}(\text{lab}) = 125^\circ$ and 78° with respect to the beam direction in 0.22-MeV steps from $E_{\text{c.m.}} = 8.5$ to 17.2 MeV and in 0.44-MeV steps from $E_{\text{c.m.}} = 17.2$ to 26.8 MeV. The large Doppler shift at 125° allows a clean separation between prompt and delayed (mainly due to β decay) components for several γ transitions of interest to our work [e.g., the $^{24}\text{Mg} 4^+ - 2^+$ 2754.2-keV transition].

Strong γ transitions originating from the residual nuclei ^{28}Si , ^{28}Al , ^{27}Al , ^{26}Mg , ^{25}Mg , ^{24}Mg , ^{24}Na , ^{23}Na , ^{21}Ne , and ^{20}Ne have been observed. Figure 1(a) shows the lower-energy portion of a sample spectrum obtained at $E_{\text{c.m.}} = 11.2$ MeV. Excitation functions for most transitions are found to be smooth and structureless. However, the excitation function for the $\alpha + ^{25}\text{Mg}$ channel, represented by the $^{25}\text{Mg} \frac{1}{2}^+ - \frac{5}{2}^+$ 585.1-keV transition exhibits quite distinct structures [Fig. 2(a)] in the lower bombarding energy region where our data points are dense. Since this transition lies close in energy to the $^{74}\text{Ge}(n, n')$ 596-keV peak, caution has been taken in analyzing the data by comparing results from different peak extraction procedures. Results from these comparisons agree with each other within errors. The analysis of the weaker $^{25}\text{Mg} \frac{3}{2}^+ - \frac{1}{2}^+$ 389.7-MeV transition also supports the above conclusion.

For the $^{12}\text{C} + ^{18}\text{O}$ reaction, γ rays were detected at $\theta_{\gamma}(\text{lab}) = 90^\circ$ in 0.5-MeV steps from $E_{\text{c.m.}} = 6.1$ to 23 MeV and in 1.0-MeV steps between 23 and 27 MeV. The medium-energy portion of a sample spectrum obtained at $E_{\text{c.m.}} = 15$ MeV is shown in Fig. 1(b).

Depending on the bombarding energy range, the $2n + ^{28}\text{Si}$, $\alpha n + ^{25}\text{Mg}$, $\alpha 2n + ^{24}\text{Mg}$, and $2\alpha + ^{22}\text{Ne}$

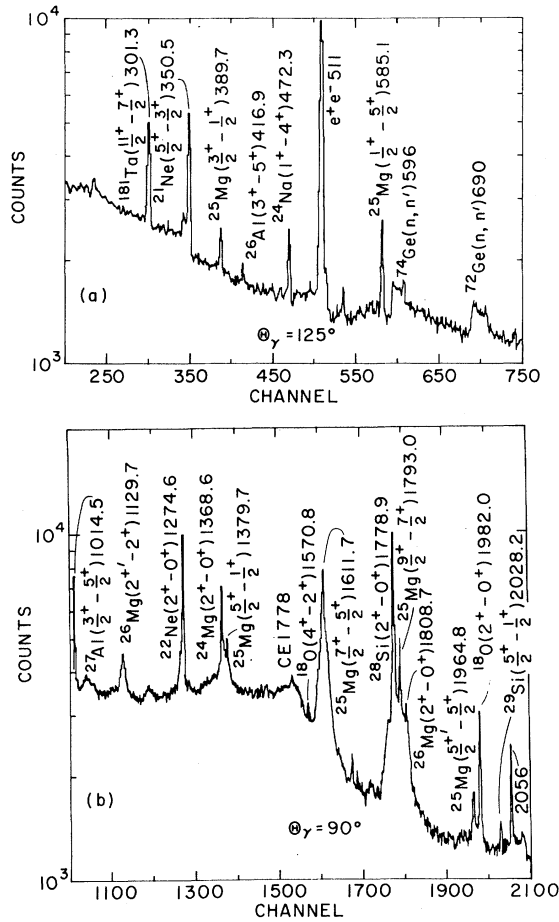


FIG. 1. γ -energy spectra showing regions of interest for (a) $^{13}\text{C} + ^{16}\text{O}$ at $E_{c.m.} = 11.2$ MeV and (b) $^{12}\text{C} + ^{18}\text{O}$ at $E_{c.m.} = 15$ MeV. γ energies are given in keV. (CE = Compton edge).

channels dominate the reaction cross section. None of the excitation functions for the stronger transitions resulting from particle evaporation display significant structures on the gross scale as compared to the α -out channels in $^{12}\text{C} + ^{16}\text{O}$ and $^{13}\text{C} + ^{16}\text{O}$. In particular, the $\alpha + ^{26}\text{Mg}$ exit channel, as represented by the $^{26}\text{Mg} 2^+ - 2^+$ 1129.7-keV transition, is structureless in contrast to the $^{12}\text{C} + ^{16}\text{O}$ and $^{13}\text{C} + ^{16}\text{O}$ reactions [Fig. 2(a)]. We have had to use the non-yrast $2^+ - 2^+$ transition in ^{26}Mg for the α -out channel in $^{12}\text{C} + ^{18}\text{O}$ rather than the yrast $2^+ - 0^+$ transition used in the $^{12}\text{C} + ^{16}\text{O}$ system since in the case of ^{26}Mg the $2^+ - 0^+$ 1808.7-keV transition is obscured by other transitions [Fig. 1(b)] and the $4^+ - 2^+$ 2510.9-keV transition is too weak to be analyzed and may also be contaminated by another ^{27}Al and ^{21}Ne transitions. It appears however that non-yrast transitions can re-

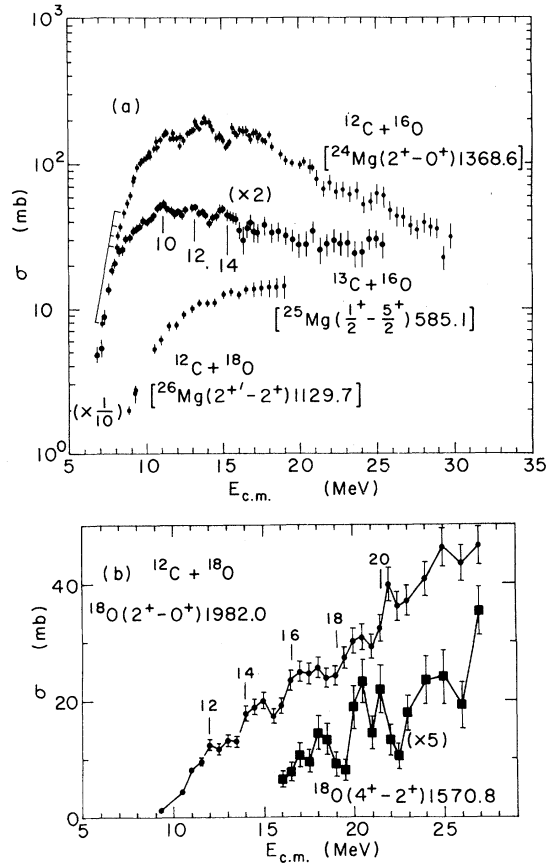


FIG. 2. (a) Comparison of structures in α -out channels for $^{12}\text{C} + ^{16}\text{O}$, $^{13}\text{C} + ^{16}\text{O}$, and $^{12}\text{C} + ^{18}\text{O}$. (b) Structures observed in the $^{18}\text{O} 2^+ - 0^+$ 1982.0-keV and the $^{18}\text{O} 4^+ - 2^+$ 1570.8-keV transitions. The solid line serves to guide the eye only.

flect structure in the fusion cross section, as evidenced by the structure in the $^{25}\text{Mg} \frac{1}{2}^+ - \frac{5}{2}^-$ transition in $^{13}\text{C} + ^{16}\text{O}$. A comparison of the excitation function (not shown) for yrast transitions for the two α -out channels in the three systems also shows an absence of structure for $^{12}\text{C} + ^{18}\text{O}$ and increasingly greater structure for $^{13}\text{C} + ^{16}\text{O}$, and for $^{12}\text{C} + ^{16}\text{O}$.²⁻⁵ The excitation function for the $^{18}\text{O} 2^+ - 0^+$ 1982.0-keV transition resulting from the inelastic excitation of the projectile, however, exhibits pronounced gross structures [Fig. 2(b)] with peaks centered at $E_{c.m.} \approx 12, 14.5, 17.3, 20$, and possibly 22 MeV. Correlated structures are also apparent in the excitation function for the weaker $^{18}\text{O} 4^+ - 2^+$ 1570.8-keV transition [Fig. 2(b)] which could be observed for $E_{c.m.} > 15$ MeV. These results are in good agreement with a recent measurement by Freeman and Haas.⁶

It is known from previous studies of the $^{12}\text{C} + ^{16}\text{O}$ system²⁻⁵ and our present $^{13}\text{C} + ^{16}\text{O}$ γ data that the α -out channel plays an important role in probing gross structures in fusion channels, especially in the lower-bombarding-energy region, where single-particle emission is a major mode of de-excitation. Results for the three α -out channels are summarized in Fig. 2(a). One observes the most pronounced structure in the $^{12}\text{C} + ^{16}\text{O}$ system, but less structure in $^{13}\text{C} + ^{16}\text{O}$ (with the addition of a $p_{1/2}$ neutron), and apparently no structure in $^{12}\text{C} + ^{18}\text{O}$ (with the addition of two $d_{5/2}$ neutrons), indicating a systematic attenuation of structure as more neutrons are added to the more tightly bound α -cluster nuclei comprising the system exhibiting the most structure. The absence of structure in the $^{12}\text{C} + ^{18}\text{O}$ system as well as the $^{12}\text{C} + ^{19}\text{F}$ systems had been noted previously.^{1,6} The fact that α -out channels exhibit the most structure and that α emission is favored for high-spin compound states supports the picture that peripheral partial waves populating the higher-spin states of the compound nucleus are mainly responsible for the observed gross structures in fusion between the p -shell nuclei.

There is evidence from the periodicity of the structure observed in the excitation functions for the preferential fusion of grazing waves of a particular parity. In case of $^{12}\text{C} + ^{16}\text{O}$, it can be deduced⁵ from the absolute values of the fusion cross section that peaks in the excitation functions occur at energies where the highest partial wave completely absorbed is even, with a change of two units of angular momentum in going from one peak to another. From Fig. 2(a), the energy spacing between peaks in the ^{25}Mg ($^{13}\text{C} + ^{16}\text{O}$) curve is comparable to that of ^{24}Mg , which suggests that the angular momentum values for structures in ^{25}Mg also differ by two units. We could not find an experimentally based global optical potential for $^{13}\text{C} + ^{16}\text{O}$ in the appropriate energy range, but as a crude estimate, we have calculated the grazing angular momenta l_g by using radially scaled potential parameters deduced from the elastic scattering of $^{12}\text{C} + ^{18}\text{O}$ by Webb.⁷ This potential also fits qualitatively the 90° elastic excitation function data of Gobbi *et al.*⁸ for $^{13}\text{C} + ^{16}\text{O}$ at lower bombarding energies. The observed spacing between peaks corresponds to a difference of two units in the grazing angular momentum.

A similar difference in the grazing angular momenta is also implied by the spacing of structures in the inelastic excitation function for the ^{18}O 2^+ -

0^+ 1982.0-keV transition in $^{12}\text{C} + ^{18}\text{O}$. The optical potential deduced by Webb⁷ for $^{12}\text{C} + ^{18}\text{O}$ has been used to calculate the energy location of grazing partial waves for this system and the result indicated in Fig. 2(b) supports a periodicity of two units of angular momentum. A parity-dependent absorption mechanism for these reactions is strongly suggested by these considerations.

The similarity of structures in the $\alpha + ^{24}\text{Mg}$ ($^{12}\text{C} + ^{16}\text{O}$) and $\alpha + ^{25}\text{Mg}$ ($^{13}\text{C} + ^{16}\text{O}$) channels may support the picture of persistence of structures in going from an active system to its neighbors. There are some indications that such a mechanism is present in the $^{13}\text{C}(^{16}\text{O}, ^{17}\text{O})^{12}\text{C}$ channel in relation to the 19.7-MeV intermediate-width structure in $^{12}\text{C} + ^{16}\text{O}$.⁹ If one evokes the fusion-through-doorways model, structures in the fusion cross section for $^{12}\text{C} + ^{16}\text{O}$ can be thought of as due to the formation of fusion doorway states in the entrance channel, with these states, plus an extra neutron, forming new doorway configurations for $^{13}\text{C} + ^{16}\text{O}$ so that the structures are to a certain extent preserved. However, as more neutrons are added to the system, the increased degrees of freedom can cause strong mixing and overlapping between these states and eventually the structures get damped away. Another indirect consequence of the added neutrons is a change in the Q -value for compound-nucleus formation, resulting in the compound-nucleus excitation energy (corresponding to a given grazing orbital angular momentum) increasing as one goes from the $^{12}\text{C} + ^{16}\text{O}$ to the $^{13}\text{C} + ^{16}\text{O}$ and $^{12}\text{C} + ^{18}\text{O}$ systems. This increases the corresponding compound-nuclear level density and hence the spreading width of the doorways. These considerations are consistent with the observed differences in the amplitude of structures in the α -out channels for the three reactions discussed above [Fig. 2(a)]. It would be interesting to have more experimental data addressed to these questions so that the above picture could be tested. Another important question to be answered is how and why the structures are distributed among the fusion and direct channels.

This work was supported in part by the U. S. Department of Energy.

(a) Permanent address: Physik-Department E12, Technische Universität München, D-8046 Garching, Federal Republic of Germany.

(b) Permanent address: Hahn-Meitner Institut, D-

1000, Berlin, Federal Republic of Germany.

^(c)Permanent address: Sektion Physik der Universität München, D-8046 Garching, Federal Republic of Germany.

¹P. Sperr, S. Vigdor, Y. Eisen, W. Henning, D. G. Kovar, T. R. Ophel, and B. Zeidman, *Phys. Rev. Lett.* **36**, 405 (1976); P. Sperr, T. H. Braid, Y. Eisen, D. G. Kovar, F. W. Prosser, Jr., J. P. Schiffer, S. L. Tabor, and S. Vigdor, *Phys. Rev. Lett.* **37**, 321 (1976).

²J. J. Kolata, R. M. Freeman, F. Haas, B. Heusch, and A. Gallmann, *Phys. Lett.* **65B**, 333 (1976); J. J. Kolata, R. C. Fuller, R. M. Freeman, F. Haas, B. Heusch, and Gallmann, *Phys. Rev. C* **16**, 891 (1977).

³Z. E. Switkowski, H. Winkler, and P. R. Christensen,

Phys. Rev. C **15**, 449 (1977).

⁴S. L. Tabor, Y. Eisen, D. G. Kavor, and Z. Vager, *Phys. Rev. C* **16**, 673 (1977).

⁵Y.-d. Chan, H. Bohn, R. Vandenbosch, K. G. Bernhardt, J. G. Cramer, R. Sielemann, and L. Green, *Nucl. Phys.* **A303**, 500 (1978).

⁶R. M. Freeman and F. Haas, *Phys. Rev. Lett.* **40**, 927 (1978).

⁷M. P. Webb, Ph.D. thesis, University of Washington, 1976 (unpublished).

⁸A. Gobbi, U. Matter, J.-L. Perrenoud, and P. Marmier, *Nucl. Phys.* **A112**, 537 (1968).

⁹P. T. Debevec, H. J. Körner, and J. P. Schiffer, *Phys. Rev. Lett.* **31**, 171 (1973).

Second-Order Excitation in Nucleus-Nucleus Interaction Potential

Bikash Sinha

Nuclear Physics Division, Bhabha Atomic Research Centre, Bombay 400 085, India

(Received 7 November 1978)

The second-order interaction potential has been calculated for two colliding nuclei where target excitation is induced by the interaction between a nucleon and the incoming self-consistent one-body field of the projectile. The real part of the second-order term is insignificant for distances larger than the touching radius, but significant for smaller distances. The imaginary potential agrees favorably with phenomenological results.

In recent years the first-order nucleus-nucleus interaction potential has been derived either by double folding the nuclear density distributions of the nuclei with a suitable two-body effective interaction¹ or by single folding a nucleon-nucleus potential with the target/projectile density distribution.² In the first instance the nuclear saturation effect can be incorporated effectively by using a suitable two-body interaction.^{1,3} In the single-folding case, the phenomenological free-nucleon-nucleus potential is folded in with the nucleon density distribution to derive the nucleus-nucleus interaction potential.²

It is apparent that in neither of the cases are all the Pauli exchange effects included. Using a reasonable effective interaction might guarantee nuclear saturation but the model does not incorporate exchange effects. The single-folding procedure has the further drawback of ignoring saturation. Pauli exchange corrections are primarily of two kinds—the antisymmetrization of the interaction matrix element and the Pauli distortion effect, which necessarily tends to increase the internal kinetic energy of the system at the expense of the relative-motion kinetic energy. The blocking of the intrinsic states of the colliding nuclei leads to the excitation of the nu-

clei. Mosel⁴ has shown the importance of including the distortion effect for a correct evaluation of the interaction potential.

The two exchange effects just mentioned have been estimated recently by various authors, employing a range of techniques and models.⁴⁻⁶ Recently the exchange effects were estimated by folding in the two density matrices of the interacting nuclei,⁷ whereas the direct part was computed by folding in the diagonal part of the density matrices—essentially in the spirit of the sudden approximation. The generalized folding procedure just described has an added advantage: One can self-consistently extract a nucleon-nucleus potential which when folded in with the target/projectile density distributions reproduces by definition the direct plus exchange total interaction potential. The self-consistent nucleon-nucleus potential in this method has all the Pauli effects built into it. It was noted that such a potential deviates from a free-nucleon-nucleus potential considerably, as expected,⁷ becoming weaker with increasing overlap of the two densities.

One inescapable manifestation of Pauli exchange is a shallow potential, which turns repulsive at short intranuclear distance, a fact not of great practical importance since the very concept of a